



Nanoscale

Electronic Supporting Information for

Fluorescent boronate-based polymer nanoparticles with reactive oxygen species (ROS)-triggered cargo release for drug-delivery applications

Eliezer Jäger,^{a,*} Anita Höcherl,^{a,*} Olga Janoušková,^a Alessandro Jäger,^a Martin Hrubý,^a Rafal Konefal,^a Miloš Netopilik,^a Jiří Pánek,^a Miroslav Šlouf,^a Karel Ulbrich^a and Petr Štěpánek^a

^a Institute of Macromolecular Chemistry v.v.i., Academy of Sciences of the Czech Republic, Heyrovsky Sq. 2, 162 06 Prague 6, Czech Republic.

Email: jager@imc.cas.cz; hocherl@imc.cas.cz

Tel: +420 296 809 322;

Materials:

Propargyl bromide solution (~ 80% in toluene), 2,6-bis-(hydroxymethyl)-*p*-cresol (95 %), imidazole (≥ 99.5 %), tert-butyltrimethylsilyl chloride (97 %), anhydrous pyridine anhydrous (99.8 %), triethylamine (≥ 99.5 %) Nile Red (microscopy grade), 2,7-dichlorodihydrofluorescein diacetate and copper (I) iodide (99.999 %) were obtained from Sigma-Aldrich (Czech Republic, CZ) and were used without further purification. Pimeloyl chloride 98 % (Sigma-Aldrich/CZ) was distilled under reduced pressure right before use. Alexa Fluor[®] 647 was purchased from Life Technologies (Czech Republic, CZ). Paclitaxel was purchased from Aurisco (China). All solvents, unless otherwise stated, were used without further purification. PC-3, HeLa, HF and DLD1 cells were obtained from American Type Cell Culture (ATCC) and cultured according ATCC guidelines.

¹H NMR and ¹³C NMR Instruments

¹H NMR and ¹³C NMR spectra of the monomers (300 and 600 MHz, respectively) were obtained using a Bruker Avance DPX 300 MHz NMR spectrometer or Bruker 600 MHz NMR spectrometer with CDCl₃ or *d*₆-DMSO as solvents at 25 °C and at 37 °C for polymer degradation studies. The chemical shifts are relative to TMS using hexamethyldisiloxane (HMDSO, 0.05 and 2.0 ppm from TMS in ¹H NMR and ¹³C NMR spectra, respectively) as internal standard. Chemical shifts as, δ , in units of parts per million (ppm).

¹H NMR and ¹³C NMR measurements of the polymer degradation

15 mg of the polymer P-1 were added into 600 μ L of *d*₆-DMSO followed by the addition of 160 μ L of deuterated PBS (pH 7.4) buffer solution. The solution was transferred to a NMR tube and incubated at 37 °C. To the solution, 40 μ L of H₂O₂ (30 % w/w solution in H₂O; Sigma-Aldrich - CZ) was added to make a 50 mM solution (in analogy to Almuatiri *et al.*, 2012).¹

Size exclusion chromatography (SEC) analysis

The weight-average molecular weight (M_w), number-average molecular weight (M_n) and the respective polydispersity $I = (M_w/M_n)$ were obtained by size exclusion chromatography (SEC) analysis. The SEC of the isolated polymers was performed at 25 °C with two PLgel MIXED-C columns (300 \times 7.5 mm, SDV gel with particle size 5 μ m;

Polymer Laboratories, USA) and with UV (UVD 305; Watrex, Czech Republic) and RI (RI-101; Shodex, Japan) detectors. *N,N*-Dimethylformamide (Sigma-Aldrich, Czech Republic) with LiBr (0.01 % v/v) was used as a mobile phase at a flow rate of 1 mL·min⁻¹. The molecular weight values were calculated using Clarity software (Dataapex, Czech Republic). Calibration with PMMA standards was used.

SEC analysis of polymer degradation.

P-1 and P-2 polymers solutions were prepared by dissolving 6 mg of the polymers in a mixture of 1.625 mL of DMF-PBS (pH 7.4, 80/20 v/v). The aqueous H₂O₂ (30 % w/w solution in H₂O) was added to reach the final hydrogen peroxide concentration of 200 μM, 500 μM, 1 mM and 5 mM, respectively. Aliquots of 250 μL were taken after 24 h, 1 day, 3 days and 4 days, respectively and evaporated to dryness. The DMF (350 μL, containing 0.01 % LiBr) was added and the filtered solutions (0.22 μM PVDF, Millipore® – Czech Republic) were injected (20 μL) into the SEC instrument. No hydrolysis in the absence of H₂O₂ of the tested polymers over 4 days was observed.

Scattering techniques

The dynamic light scattering (DLS) measurements were performed using an ALV CGE laser goniometer consisting of a 22 mW HeNe linear polarized laser operating at a wavelength ($\lambda = 632.8$ nm), an ALV 6010 correlator, and a pair of avalanche photodiodes operating in the pseudo cross-correlation mode. The samples were loaded into 10 mm diameter glass cells and maintained at 25 ± 1 °C. The data were collected using the ALV Correlator Control software and the counting time was 30 s. The measured intensity correlation functions $g_2(t)$ were analysed using the algorithm REPES² resulting in the distributions of relaxation times shown in equal area representation as $\tau A(\tau)$. The mean relaxation time or relaxation frequency ($\Gamma = \tau^{-1}$) is

related to the diffusion coefficient (D) of the nanoparticles as $D = \frac{\Gamma}{q^2}$ where $q = \frac{4\pi n \sin \frac{\theta}{2}}{\lambda}$ is the scattering vector with n the refractive index of the solvent and θ the scattering angle. The hydrodynamic radius (R_H) or the distributions of R_H were calculated by using the well-known Stokes-Einstein relation:

$$R_H = \frac{k_B T}{6\pi\eta D} \quad (\text{eq. S1})$$

with k_B the Boltzmann constant, T the absolute temperature and η the viscosity of the solvent.

The polydispersity of the nanoparticles was accessed by using the cumulant analysis² of the correlation functions measured at 90° as:

$$\ln g_1(t) = \ln C - \Gamma t + \frac{\mu_2}{2} t^2 \dots \quad (\text{Eq. S2})$$

wherein C is the amplitude of the correlation function and Γ is the relaxation time (τ^{-1}). The parameter μ_2 is known as the second-order cumulant and it was used to compute the polydispersity index of the samples ($\text{PDI} = \mu_2/\Gamma^2$).

In the static light scattering (SLS), the scattering angle was varied from 30 to 150° with a 10° stepwise increase. The absolute light scattering is related to weight-average molar mass ($M_w(\text{NP})$) and to the radius of gyration (R_G) of the nanoparticles by the Zimm formalism represented as:

$$\frac{K_c}{R_\theta} = \frac{1}{M_w(\text{NP})} \left(1 + \frac{R_G^2}{3} q^2 \right) \quad (\text{eq. S3})$$

where K is the optical constant which includes the square of the refractive index increment (dn/dc), R_θ is the excess normalized scattered intensity (toluene was applied as standard solvent) and c is the polymer concentration given in $\text{mg}\cdot\text{mL}^{-1}$. The refractive index increment (dn/dc) of the P-1 NPs in PBS ($0.148 \text{ mL}\cdot\text{g}^{-1}$) was determined using a Brice-Phoenix differential refractometer operating at $\lambda = 632.8 \text{ nm}$.

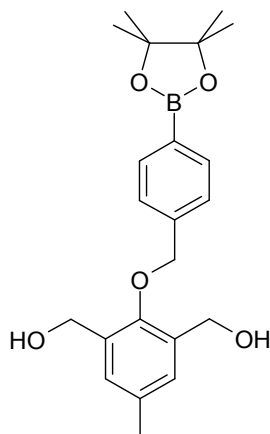
Transmission electron microscopy (TEM)

The TEM observations were carried out on a Tecnai G2 Spirit Twin 120kV (FEI, Czech Republic). Two microliters of P-1 NPs ($1 \text{ mg}\cdot\text{mL}^{-1}$; 1 mM of H_2O_2 for the P-1 after 48 h incubation) were dropped onto a copper TEM grid (300 mesh), which was coated with thin, electron-transparent carbon film. After 1 min the solution was sucked out by touching the bottom of the grid with filtering paper. This fast removal of the solution was performed in order to minimize oversaturation during the drying process; this step was found necessary to preserve the structure of nanoparticles. The NPs were negatively stained with uranyl acetate ($2 \mu\text{L}$ of $1 \text{ wt.}\%$ solution dropped onto the dried nanoparticles and sucked out after 1 min, using the same way that was described above). The sample was left to dry completely at ambient temperature and then observed in the TEM microscope using bright field imaging. Under these conditions, the micrographs display dark, negatively stained background with bright spots, which correspond to the investigated nanoparticles.

Synthesis of the polymer precursors and monomers

Synthesis of the monomer 1

The monomer 1 and its precursors were synthesized according previously published methodology of Almutairi *et. al.*, 2012.¹



¹H NMR (CDCl₃): δ 7.89 (d, 2H), 7.49 (d, 2H), 7.22 (s, 2H), 5.03 (s, 2H), 4.73 (s, 4H), 2.39 (s, 3H), 1.74 (s, 2H), 1.42 (s, 12H). ¹³C NMR (CDCl₃): δ 152.86, 140.01, 135.32, 134.65, 134.03, 129.83, 127.34, 84.05, 76.73, 61.31, 25.02, 20.99.

Synthesis of the monomer 2

Synthesis of the precursor 1: 2,6-Bis-(hydroxymethyl)-*p*-cresol (10 g, 57.7 mmol) and imidazole (8.90 g, 130.7 mmol) were dissolved in 40 mL of dry DMF and cooled to 0°C. *tert*-Butyldimethylsilyl chloride (TBDMSCl) (19.72 g, 126.9 mmol) dissolved in 30 mL of dry DMF was added dropwise. The reaction mixture was stirred for 2 h at room temperature and monitored by TLC by using hexane-ethyl acetate (95:5) v/v as a mobile phase. After completion, the reaction mixture was diluted with Et₂O and the organic layer was washed 3 times with water. The organic layer was separated, dried over Na₂SO₄ and evaporated under reduced pressure. The crude product was purified by flash-chromatography on silica gel using hexane-ethyl acetate (95:5) v/v as a mobile phase to give **compound 1** (21.65 g, 95 %) as a colorless oil.

^1H NMR (CDCl_3): δ 7.89 (*d*, 2H), 7.49 (*d*, 2H), 7.22 (*s*, 2H), 5.03 (*s*, 2H), 4.73 (*s*, 4H), 2.39 (*s*, 3H), 1.74 (*s*, 2H), 1.42 (*s*, 12H). ^{13}C NMR (CDCl_3): δ 152.86, 140.01, 135.32, 134.65, 134.03, 129.83, 127.34, 84.05, 76.73, 61.31, 25.02, 20.99.

Synthesis of the precursor 2: To a stirred suspension of the precursor 1 (5.59 g, 14.1 mmol) and potassium carbonate (5.0 g, 36.2 mmol) in DMF (20 mL) was added propargyl bromide (1.9 mL, 16 mmol, 80% solution in toluene) and the reaction mixture was stirred for 12 h at room temperature. The reaction mixture was quenched with H_2O (200 mL) and extracted with Et_2O (3 x 50 mL). Combined extracts were washed with aqueous NaCl solution (10 wt.%, 2 x 50 mL), dried over MgSO_4 , and solvent was removed under vacuum. The residue was purified by flash column chromatography (gradient elution 20:1 \rightarrow 15:1 hexanes:ethyl acetate) to afford precursor 2 (5.86 g, quantitative) as a yellow liquid.

^1H NMR (300 MHz, CDCl_3): δ 6.93 (*d*, $J = 8.8$ Hz, 2H), 6.85 (*d*, $J = 8.8$ Hz, 2H), 4.64 (*d*, $J = 2.2$ Hz, 2H), 3.77 (*s*, 3H), 2.51 (*t*, $J = 2.4$ Hz, 1H); ^{13}C NMR (300 MHz, CDCl_3) δ 154.5, 151.7, 116.1, 114.6, 78.9, 75.3, 56.6, 55.7.

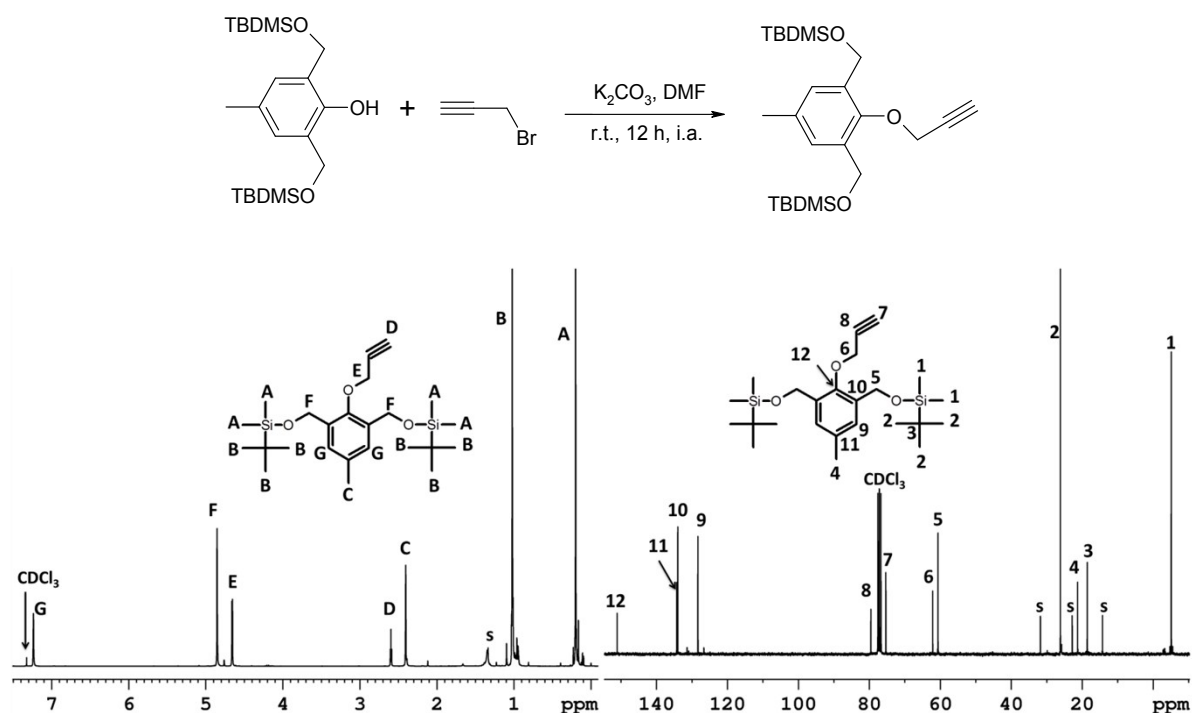


Fig. S1.: ^1H NMR (left) and ^{13}C NMR (right) of the synthesized precursor 2.

Removal of the protecting group of the precursor 2

Precursor 2 (2.5 g, 5.75 mmol) was dissolved in 10 mL of methanol. Catalytic amount of pTsOH was added. The reaction mixture was stirred at room temperature overnight and monitored by TLC (Hex/EtOAc 1:1). After completion of the conversion, the solvent was removed under reduced pressure. The product was purified by chromatography on silica gel (hexane-ethyl acetate 1:1 v/v) to give monomer 2 (1.12 g, 94 %) as a white solid.

^1H NMR (DMSO): δ 7.18 (s, 2H), 5.08 (s, 2H), 4.61 (d, 2H), 4.57 (s, 4H), 3.59 (t, 1H), 2.32 (s, 3H). ^{13}C NMR (DMSO): δ 151.07, 135.41, 133.53, 128.28, 80.51, 78.64, 62.01, 58.64, 21.32.

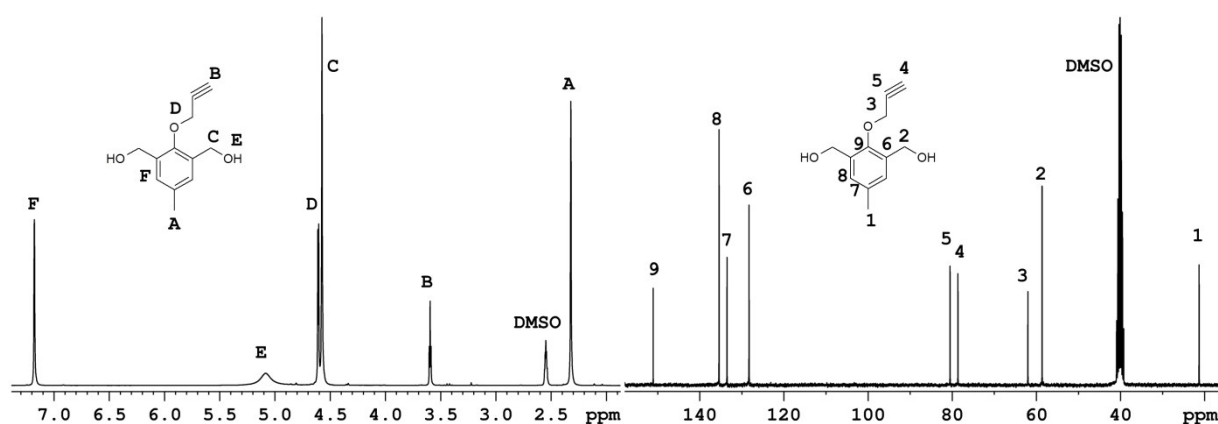


Fig. S2.: ^1H NMR (left) and ^{13}C NMR (right) of the synthesized monomer 2.

Synthesis of the polymer 1

To a *N,N*-dimethylacetamide (DMA) solution of the synthesized monomer 1 (576 mg, 1.5 mmol), monomer 2 (288.32 mg, 1.5 mmol) and pyridine (3.0 mL, 37 mmol), pimeloyl chloride (591.2 mg, 3 mmol) in DMA (25 mL) was added dropwise over 10 minutes at room temperature. The reaction was stirred at room temperature for 24 h. The slurry was then dialyzed (Spectra/Por dialysis membrane, 6-8 kD MWCO) for 72h in water (water changed after every 12h). The precipitate was further purified by dissolution in dichloromethane (DCM) and precipitation into cold

EtOH. The polymer was recovered and dried under vacuum (48 h) (1.25 g, 72 %) being obtained as a yellow solid. Weight-average molecular weight (M_w), number-average molecular weight (M_n) and polydispersity index (PDI) of the synthesized polymer was determined to be 21 500 Da (M_w), 14 300 Da (M_n) and 1.49 (PDI), respectively, by SEC measurements using polystyrene standards (discussed hereafter).

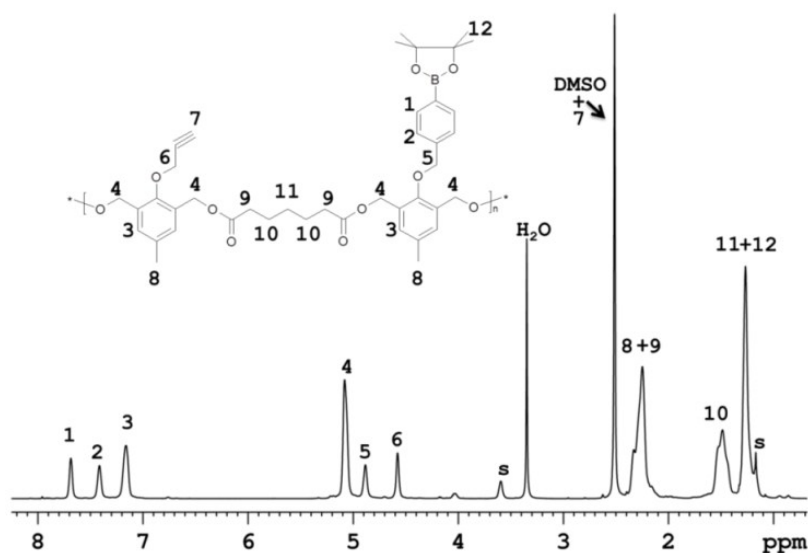


Fig. S3.: ^1H NMR of the synthesized polymer 1 (P1) in d_6 -DMSO.

Synthesis of the polymer 2

To a DMA solution of the synthesized monomer 2 (288.32 mg, 1.5 mmol) and pyridine (2.0 mL, 24.7 mmol), pimeloyl chloride (295.6 mg, 1.5 mmol) was added dropwise over 10 minutes at room temperature. The reaction was stirred at room temperature for 24 h. The slurry was then dialyzed (Spectra/Por dialysis membrane, 6-8 kD MWCO) for 72h in water (water changed after every 12h). The precipitate was further purified by dissolution in DCM and precipitation into cold EtOH. The polymer was recovered and dried under vacuum (48 h) (396.5 mg, 68 %) being obtained as a yellow solid. Weight-average molecular weight (M_w), number-average molecular weight (M_n) and polydispersity index (PDI) of the synthesized polymer was determined to be 21 200 Da (M_w), 12 900 Da (M_n) and 1.64, respectively, by SEC measurements using polystyrene standards (Fig. S5, black lines).

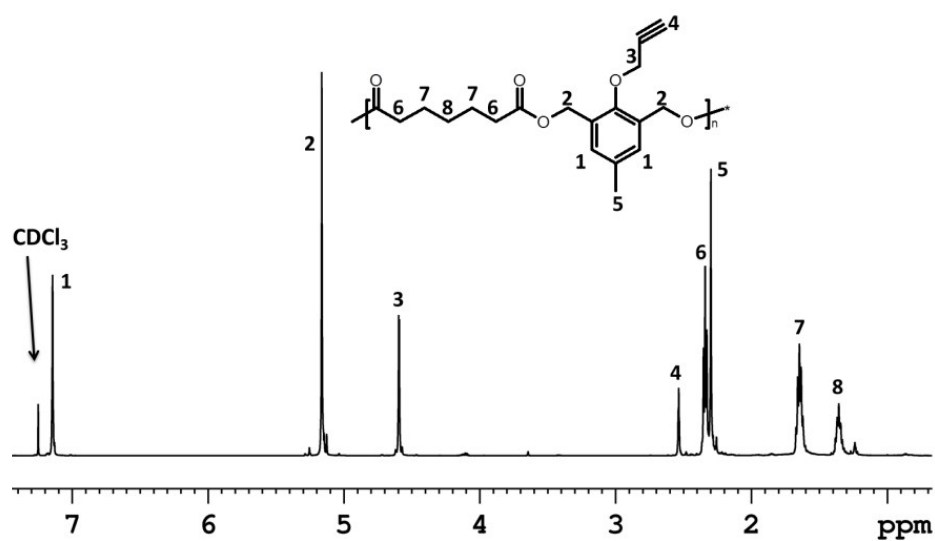


Fig. S4.: ¹H NMR of the synthesized counterpart polymer 2 (P2) in CDCl₃.

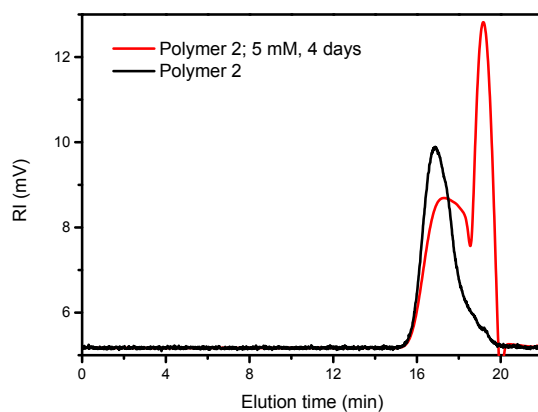
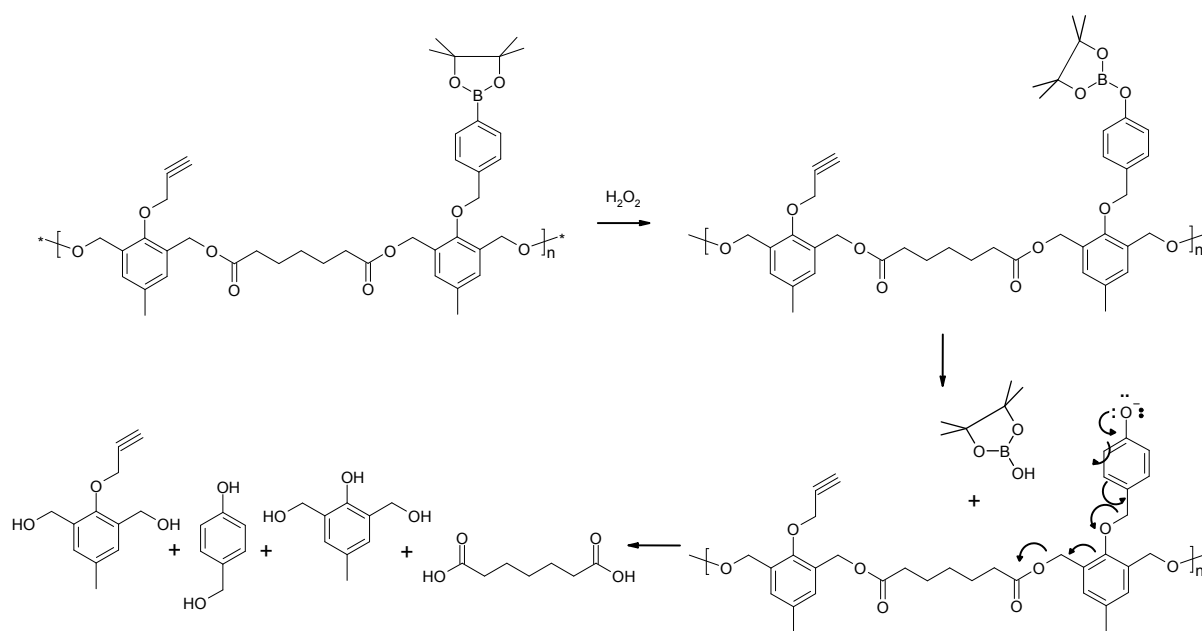
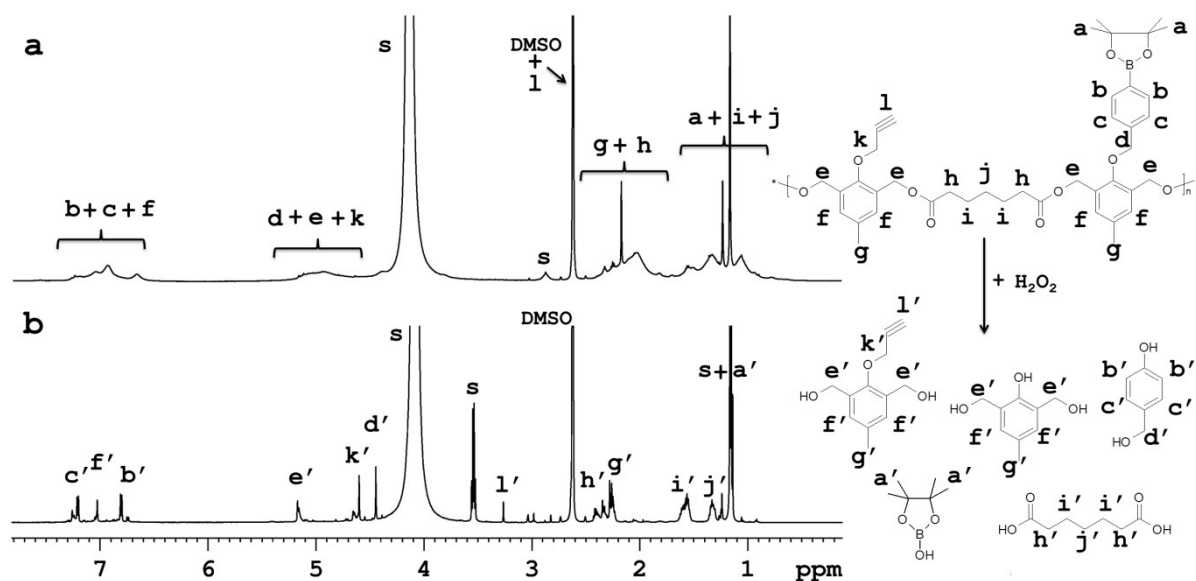


Fig. S5.: SEC chromatograms of P2 prior to the addition of H₂O₂ (black line) and after degradation in 20% PBS/DMF solutions containing 5 mM of H₂O₂ incubated at 37 °C for 4 days (red line).

Scheme S1.: Mechanism of P1 polymer degradation triggered by H₂O₂.Fig. S6.: ¹H NMR spectra of polymer 1 in *d*₆-DMSO, deuterium PBS (a) without H₂O₂ and (b) incubated with 50 mM H₂O₂ after 5 days at 37 °C. “s” refers to solvent peaks (HDO in D₂O and ethanol).

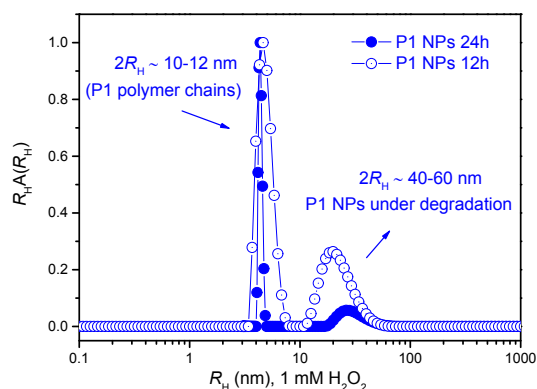


Fig. S7.: Volume-weighted distributions of R_H for P1 after 12h (○) and 24 h (●) of incubation in 1 mM of H_2O_2 .

Nile Red assays

Nile Red calibration curves

The amount of Nile Red in the P-1 and P-2 polymers was quantified by fluorescence spectroscopy (JASCO spectroscopy, Model FP-6200 Spectrofluorometer) as described below.

Nanoparticles preparation: Blank and Nile-Red (NR) loaded NPs (NR-NPs)

To 5 mL of a solution of P-1 or P-2 (20 mg) and Nile Red (50 μ g) in acetone, 10 mL of PBS (containing 0.01 % tween 80) were added as precipitant. The remaining acetone was removed by evaporation and the final volume of the NPs was concentrated to 5 mg·mL⁻¹. Afterwards the NPs solution was washed twice with PBS by using centrifugation/filtration (Amicon 10 kDa – Millipore, Czech Republic). The final NR content on the NPs was adjusted to 8.05 μ g·mL⁻¹ of NR in PBS (0.2 wt % polymers). Blank NPs were prepared by the same procedure, however, with no NR addition (Fig. 2b).

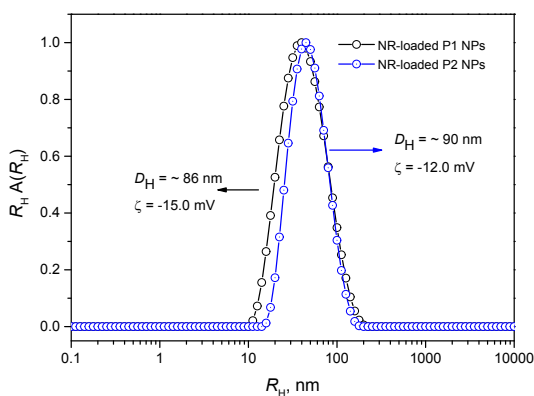


Fig.S8.: Distributions of R_H and ζ -potential values for P1 (○) and P2 (●) NR-loaded NPs.

EE determined by Nile red fluorescence.

P-1 and/or P-2 NPs encapsulating Nile red were dissolved in a mixture of acetone:H₂O (95 : 5) to release Nile red into the solution. Nile red fluorescence intensity was measured (excitation at 530 nm, emission at 605 nm) and the amount of dye encapsulated was determined according to the calibration curve presented in Fig. S8. All calibration curves were obtained by measuring fluorescence of various concentrations of Nile red in acetone. Linear regression of peak area *versus* concentration yielded the curve.

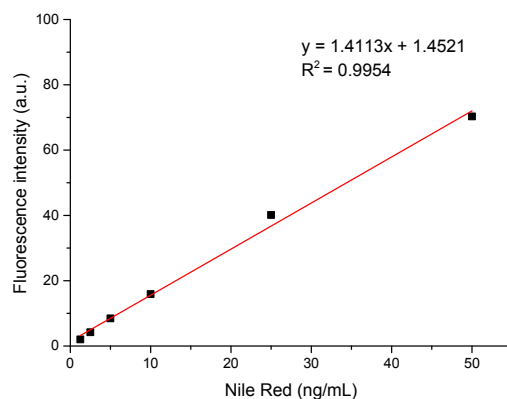


Fig. S9. Calibration curve for Nile Red fluorescence.

Nile-Red release experiments

To 5 mL vials the P-1 or P-2-loaded NR-NPs (250 μ g of polymer – 0.5 μ g NR) in PBS (pH ~ 7.4) were added and dissolved to 5 mL with PBS aqueous buffer (pH ~ 7.4). Afterwards H₂O₂ was added to reach the concentration of 1 mM and the vials were incubated at dark at 37 °C along 24 h. Aliquots were removed and directly quantified as described above. The release experiments were performed in 3 replicates at various time points. The neglected fluorescence interaction between NR and H₂O₂ was previously demonstrated by Almutari *et al.*, 2012.¹

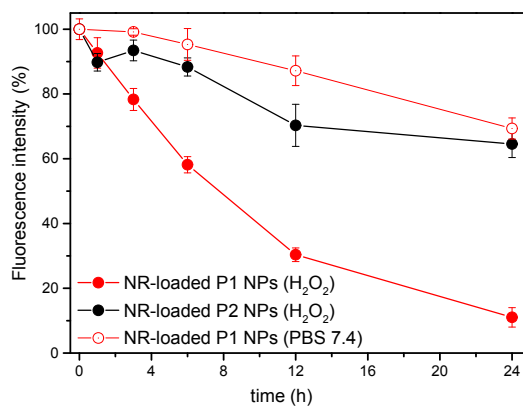


Fig. S10.: Nile Red (NR) release from the ROS-responsive P1 NPs (red filled circles) and from the ROS-non-responsive counterpart P2 NPs (black filled circles) along 24 h incubation in 1 mM H₂O₂ at 37 °C. (Open circles shows the NR release from the responsive P1 NPs in phosphate buffer saline (PBS) pH 7.4 at 37 °C along 24h).

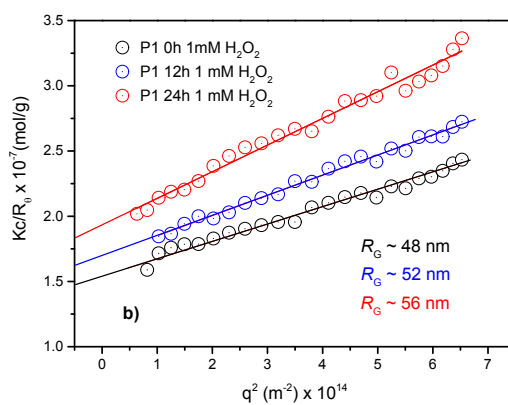
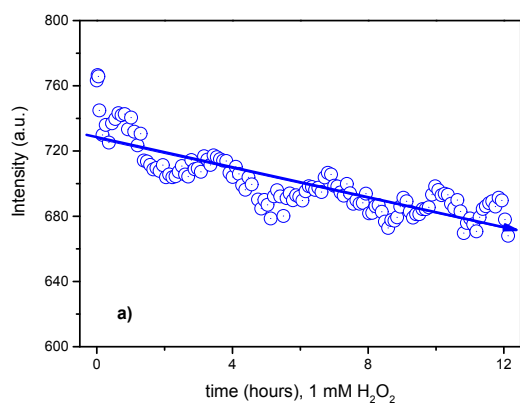


Fig. S11. Overall scattering intensity (a) and (b) static light scattering measurement (Kc/R_0 vs. q^2) for P1 NPs ($1.0 \text{ mg}\cdot\text{mL}^{-1}$) in PBS (pH ~ 7.4) under incubation with 1 mM of H_2O_2 .

Confocal Laser Scanning Microscopy (cLSM) Studies of P1 and P2 NPs internalization in cells

Microscopy data was acquired at a confocal laser scanning microscope FV10-ASV (Olympus Europe, Czech Republic) equipped with a FLIM module (PicoQuant, Germany), on a 60x oil objective. The software FV10-ASW and SymphoTime64 from Olympus and PicoQuant, respectively, was used for acquisition and analysis. $10\cdot 10^{-3}$ PC-3 cells per well were seeded in coated Ibidi® 8 well μ -slides (Ibidi, Germany) and left to adhere at least overnight.

The cells were incubated with $200 \text{ }\mu\text{g}\cdot\text{mL}^{-1}$ of Nile Red-loaded ($\sim 0.2 \text{ \% wt}$) P1 or P2 polymer NPs for 4 h or 20 h. All cells were washed after incubation and topped with PBS for visualization, containing if required $0.5 \text{ }\mu\text{g}\cdot\text{mL}^{-1}$ of Hoechst 33342 dye. The Hoechst dye (exc. 405 nm, emission in BP425/50), Nile Red (exc. 546 nm, emission in BP610/50) and transmission were visualized. After only 4 h incubation, the ROS-triggered NR release out of P1 particles could not have progressed far, with the majority of NR still entrapped inside the NPs. After 4 h incubation P1 and P2 NPs displayed, as was expected owed to the near identical nature of the particle and material, similar uptake efficiency (see Fig. S13). Therefore, the observed difference in NR fluorescence after 20 h incubation (when P1 signals were weaker than P2 signals, see Fig. S12b and S12d), the NR quenching is attributed to ROS-mediated P1 degradation and release of NR.

a**b****c****d**

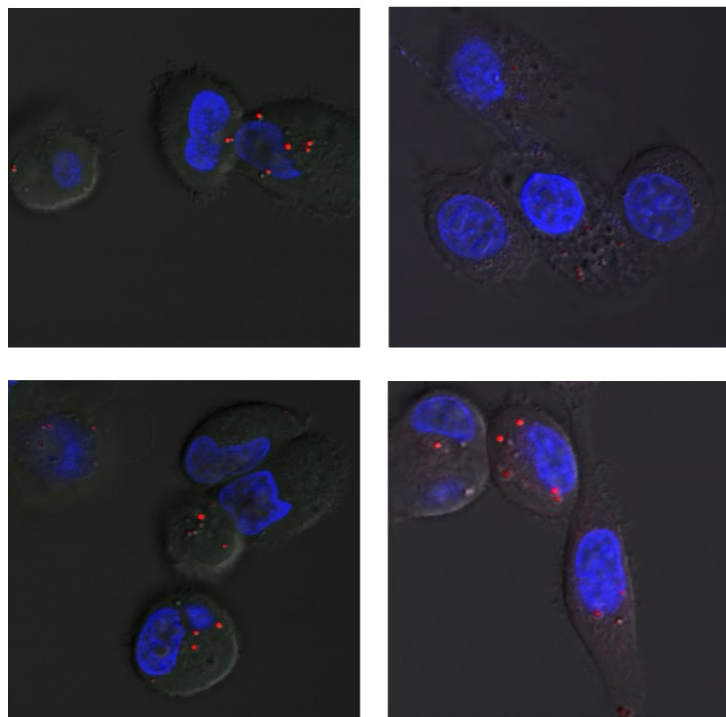


Fig. S12 Confocal microscopy images of Nile Red-loaded P1 NPs (a,b) and P2 NPs (c,d) in PC3 cells after incubation for 4 h (a,c) and 20 h (b,d) at $200 \mu\text{g}\cdot\text{mL}^{-1}$ polymer concentration. Blue the Hoechst-stained nucleus; red the NR.

Flow Cytometry (FC) analysis: In vitro release of Nile Red from internalized NPs

The FC studies were done at a BD FACSverse machine and software FlowJo (FlowJo, Oregon, US) for data analysis. The PC-3 cells were seeded in triplicate in 24 well plates, cell density $50\cdot 10^3$ per well, and left to adhere at least overnight before adding the NPs. HF cells were seeded at a density of $30\cdot 10^3$ per well. After particle incubation cells were washed, trypsinized, and prepared for analysis in PBS supplied with $0.5 \mu\text{g}\cdot\text{mL}^{-1}$ of Hoechst 33342. Hoechst was excited at 405 nm and detected in the UV channel (BP448/45), Nile Red was excited at 488 nm and detected in the PerCP-Cy5.5 channel (BP700/54). At least $10\cdot 10^3$ cells were acquired. In data analysis, after pre-gating in a fluorescence-vs-time graph (to exclude potential flow disturbances), cells were gated subsequently *via* forward scatter area-vs-height (singlet duplet distinction), and forward scatters vs UV channel (gating on live cells).

HF and PC-3 cells were incubated for 2 h with $200 \mu\text{g}\cdot\text{mL}^{-1}$ of Nile Red-loaded P1 polymer NPs and in a similar setup, PC-3 cells were loaded with NR-loaded P1 or P2 NPs. After washing with buffer, one half of the cell samples was topped with fresh incubation medium (without particles) and returned to the incubator for another 4 hours (samples 't=4h'). The other half of

samples was trypsinized immediately and proceeded to FC analysis (samples 't=0h'). Keeping the second incubation time at 4 h reduces inaccuracy potentially introduced by *e.g.*, cell division and exocytosis of the NPs.³

The NR fluorescence of P1 NPs before and after 4 h incubation was compared in HF and in PC-3 cells to track down cancer cell-specific NR quenching caused by ROS-mediated P1 degradation (*see* Fig. 4). Indeed the NR fluorescence in PC-3 cells was quenched more than in the low-ROS HF cells, indicating the triggering of specific cargo release.

Moreover a comparison of the NR fluorescence P1 and P2 NPs in PC3 cells confirmed that both NPs have the same cellular uptake efficiency (*see* Fig. S13). This provided the base for the toxicity studies, where the ROS-triggered release of PTX and the subsequent cell kill efficiency of drug-loaded P1 was compared to the non-responsive P2 NPs system.

The remaining fluorescence in P2 NPs was x 1.3 higher than the remaining NR fluorescence in P1 NPs after incubation in PC-3 cells. Therefore these findings also demonstrated that the P1 NPs can selectively release their cargo in the presence of ROS *e.g.*, to a higher extent than the non-responsive P2 NPs.

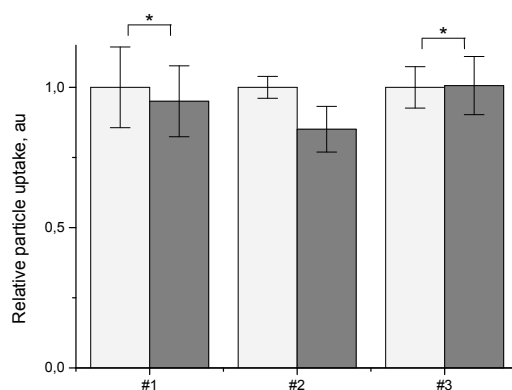


Fig. S13 Comparison of the cellular uptake of responsive P1 (grey) and non-responsive P2 (white) NPs in PC3 cells after 2 h incubation at $200 \mu\text{g}\cdot\text{mL}^{-1}$. *Equal under < 0.01 conditions in Student's t-Test.

***In vitro* release of Nile Red (NR) from NPs in PC-3 cells in presence of catalase (ROS-scavenger)**

Catalase scavenges the hydrogen peroxide and will thus prevent the peroxide-induced degradation of P1 NPs in cancer cells. In order to test the effect of a ROS scavenger on the release of NR from the ROS-responsive P1 NPs in cells, PC-3 cells were pre-incubated with catalase prior to particle addition (bovine liver catalase, Sigma Aldrich). The PC-3 cells were seeded as described and after 30h they were pre-incubated with $1 \text{ mg}\cdot\text{mL}^{-1}$ of catalase enzyme for 16 h prior to particle addition. Then the catalase content was reduced 1/5 and $200 \mu\text{g}\cdot\text{mL}^{-1}$ of NR loaded P1 or P2 NPs were added. After 8h incubation the fluorescence of NR in the cells was analysed *via* flow cytometry. An average of at least 10000 cells was detected and NR

fluorescence in the PE channel (excitation 488 nm, emission BP 586/42) was read out. The displayed data represents 5 experiments ($n=5$) done in triplicate well setup (Fig. S14).

Catalase scavenges the hydrogen peroxide which prevents the peroxide-induced degradation of P1 NPs in PC-3 cells. Therefore the P1 samples with catalase showed less NR release and subsequently less quenching of NR fluorescence. In the presence of the ROS scavenger, a significantly higher fluorescence of NR remained than in the P1 samples without the scavenger. Moreover, the fluorescence level in cells incubated with the non-responsive P2 NPs was not significantly altered by the presence of catalase.

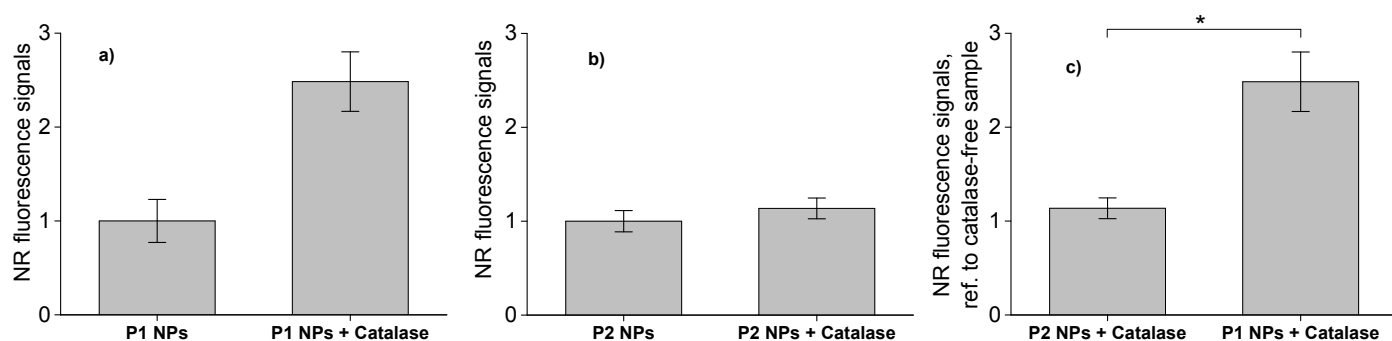


Fig. S14. Nile Red (NR) release from NR-loaded P1 and P2 NPs in presence of catalase. PC-3 cells were incubated for 8h with NR-loaded P1 (a) and P2 (b) NPs, demonstrating the effect of the ROS scavenger catalase (16 h pre-treated) on the NR signals in the cells. Figure (c) demonstrates that catalase-induce increase of NR fluorescence of P1 NPs, as opposed to the unchanged NR fluorescence in the samples with the non-responsive P2 NPs. Catalase scavenges the hydrogen peroxide which prevents the peroxide-induced degradation of P1 NPs in PC-3 cells. Therefore the P1 samples with catalase showed less NR release and subsequently less quenching of NR fluorescence. Note that the columns in (c) both represent the relative NR signal as compared to the respective samples of catalase-free incubation (shown in a, b). * Significant at $< 0,01$ (ANOVA One-Way Tukey).

Synthesis of the polymer P-1-with conjugated Alexa Fluor® 647

To a 5 mL vial equipped with a magnetic stirrer and containing dry DMF (2.5 mL) was charged polymer P1 (40 mg, 0.05 mmol terminal alkyne groups), Alexa Fluor® 647 azide dye (0.5 mg, 0.000588 mmol) and triethylamine (10 μ L, 0.05 mmol). Under argon, rapid stirring was initiated, after which copper (I) iodide (0.2 mg, 0.001 mmol) was added and the vessel was quickly sealed with a crimp teflon cap. The mixture was stirred for 5 min at room-temperature then placed on a pre-heated carousel plate and vigorously stirred at 40 °C for 6h. The reaction was cooled and filtered to aluminium column to remove cooper

catalyst. The blurry mixture was then dialyzed for 48h at dark. Afterwards the P1 polymer-Alexa Fluor® 647 conjugate was recovered by lyophilisation (31.2 mg, 78 %) being obtained as a light blue solid.

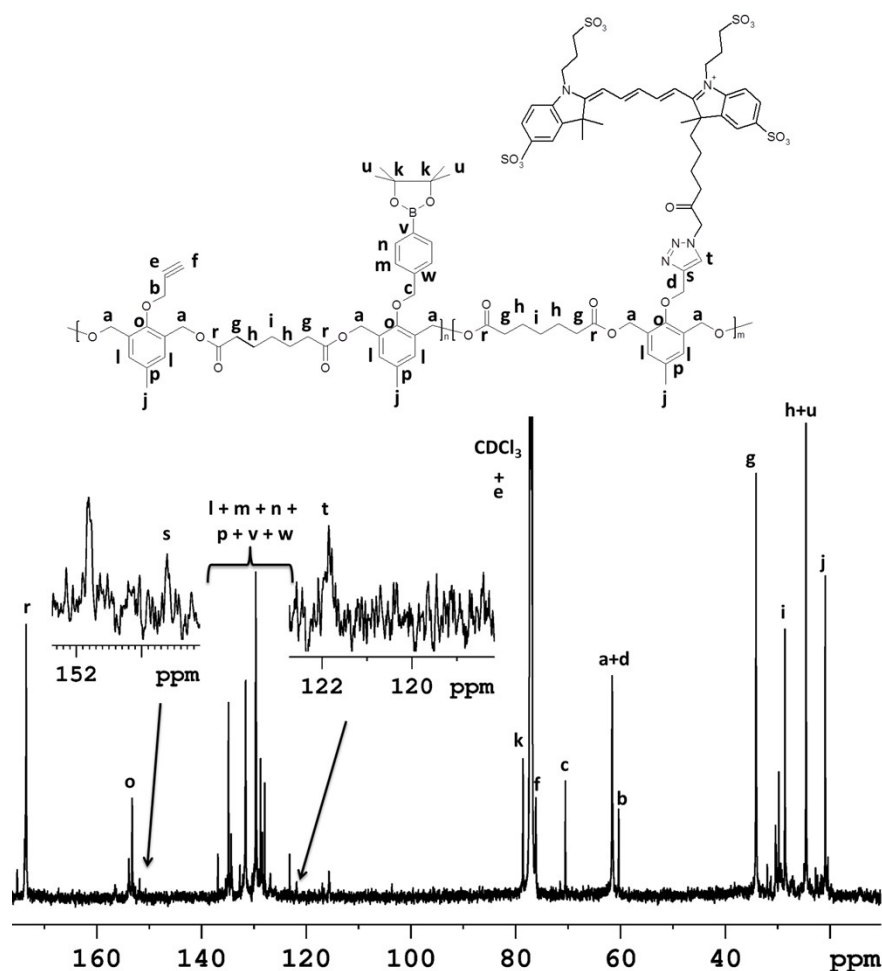


Fig. S15. ^{13}C NMR spectra of the P1 NPs covalently bonded to Alexa Fluor® 647 in CDCl_3 . The peaks corresponding to the 1,2,3-triazole ring of the linker are more than 3 times signal of background noise (proof of presence).

Preparation of NR-loaded- and Alexa Fluor® 647-bonded NPs

To 2.5 mL of a solution containing 1mg of P1 bonded Alexa Fluor + 9 mg of P1 and Nile Red (25 μg) in acetone, 5 mL of PBS (containing 0.01 % tween 80) were added as precipitant. The remaining acetone was removed by evaporation and the final volume of the NPs was concentrated to 2.5 $\text{mg}\cdot\text{mL}^{-1}$. Afterwards the NPs solution was washed twice with PBS by using centrifugation/filtration (Amicon 10 kDa – Millipore, Czech Republic). The final NR content on the NPs was adjusted to 3.75 $\mu\text{g}\cdot\text{mL}^{-1}$ of NR (Fig. S9) in PBS containing 0.082 $\mu\text{g}\cdot\text{mL}^{-1}$ of Alexa Fluor® 647 (Fig. S16).

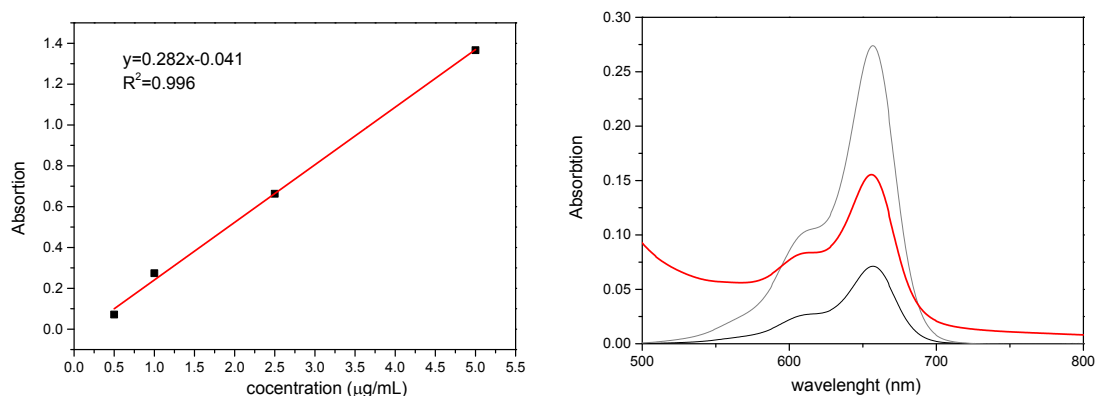


Fig. S16. Calibration curve for Alexa Fluor® 647 (left) and quantification of polymer P1 with conjugated Alexa Fluor® 647 (right – red lines) by UV-Vis spectrometer in DMF (black line corresponds to $0.25 \mu\text{g}\cdot\text{mL}^{-1}$ and grey line corresponds to $1.0 \mu\text{g}\cdot\text{mL}^{-1}$).

Microscopy: Fluorescence Lifetime Imaging (FLIM) analysis of P-1 Nile Red release in PC-3 and HF cells

As described above, microscopy studies were done using an Olympus FV10-ASV upgraded with a PicoQuant FLIM module (PicoQuant, Germany), on a 60x oil objective. The software FV10-ASW and SymphoTime64 from Olympus and PicoQuant, respectively, was used for acquisition and analysis. $10\cdot 10^{-3}$ PC-3 cells per well were seeded in coated Ibidi® 8 well μ -slides (Ibidi, Germany) and left to adhere at least overnight. Otherwise $30\cdot 10^{-3}$ cells HF per well were seeded in Poly(L-lysine)-coated 4-chamber glass bottom dishes (Cellvis, California, US).

Alexa Fluor® 647 dye was chosen for its high photostability and more even for its insensitivity to self-quenching, to changes in hydrophobicity or pH as described by the manufacturer. The short lifetime of 2.2 ns should therefore be rather constant under different conditions, providing reliable identification of Alx647 from the 2nd used dye, Nile Red. Nile Red fluorescence is most intense in hydrophobic surroundings (as *e.g.*; inside the NPs), and most quenched in hydrophilic surroundings (as *e.g.*; in cell cytoplasm). Just as the spectrum and intensity of NR fluorescence vary with external factors, the NR lifetime is equally affected. A lifetime of roughly 4.2 ns is most common for Nile Red, however its lifetime may vary between 3 and 5 ns in specific surroundings.⁴⁻⁶ Note that despite these variations NR in particular the NR released in the cell volume has at all times a lifetime that is easily distinguished from that of Alx647 in FLIM.

PC-3 and HF cells were incubated for 1h and 8h with $200 \mu\text{g}\cdot\text{mL}^{-1}$ of dual-stained (physically entrapped NR and covalently bound Alx647) P1 NPs. Cells were washed and visualized without further staining. Pretesting, data not shown here, had

identified the most suitable settings and had also ensured that under these settings, minimal cross-bleeding of the dyes and no false-positive signals (from the respective other dye, or from cell autofluorescence) occurred. Nile Red was excited with a pulsed 485 nm laser and Alx647 with a pulsed 640 nm laser, and both dyes were visualized in the red channel (Ch2 at 650/50 nm).

The dyes were first measured separately to visualize P1 NPs in PC-3 and HF cells (Fig. 5), excluding any false-positive signals from the respective other dye. Note that contributions of NR excited at 640 nm are very low and not relevant. For a better display of the co-localization (*e.g.*; colour-coded display in one image), the dyes were also measured with simultaneous excitation by both lasers – thus acquiring an image of colour-coded co-localization of the dyes in PC-3 and HF cells (Fig. 6). Areas containing predominantly one dye yield an average lifetime in each pixel that is near identical to that dye's lifetime (τ_{NR} or τ_{Alx647}). In areas where both dyes are present, photons from both dyes and therefore values of τ_{NR} and τ_{Alx647} are detected. The lifetimes of all photons per one pixel are averaged, and as a result an averaged lifetime is assigned to the pixel. The degree of dye co-localization is therefore colour-coded by averaged lifetime per pixel. A differentiation between released Nile Red (τ_{NR} *ca.* 4 ns, displayed as green), predominantly Alexa 647 (τ_{Alx647} *ca.* 2 ns, displayed as blue) and co-localization of both dyes (lifetime between 2-3 ns, displayed as green-blue) is therefore possible. It was observed that in pixels depicting internalized nanoparticles the average lifetime was close to 2, but that however two decay processes (at *ca.* 1 ns and 2 ns lifetime) were present, that correspond to Alx647 and Nile Red, respectively. As described by Jee *et al.*, in 2009,⁵ Nile Red lifetime in polymer materials is distinctly shorter than 3 ns, therefore Nile Red inside the P1 NPs has a different lifetime than the released Nile Red displaying τ of higher 4 ns. Owing to the overlapping emission spectra, such precise distinction of the different dyes and dye status would be impossible by regular microscopy based on excitation and emission wavelength.

This study showed that P1 NPs inside PC-3 cells release relatively more NR than the same particles inside HF cells, after 8 h incubation (Fig. 6). It also visible that after only 1 h incubation, the NR release from P1 NPs is low even in PC-3 cells (Fig. S17). Lifetime imaging therefore demonstrated that P1 NPs can release their cargo in a cell type- and time-dependent manner.

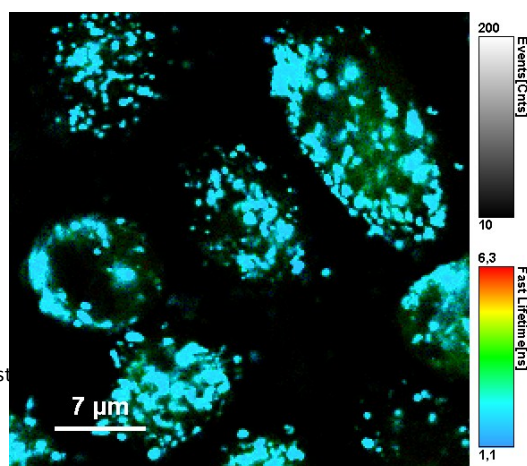


Fig. S17. FLIM images of PC-3 cells after 1 h incubation with dual-marked P1 NPs, color-coded by the averaged obtained lifetime per pixel. The localization of polymer (covalently bound Alx647, tau 2 ns, shown in blue) and of Nile Red (originally physically entrapped in the NPs, tau 4 ns, shown in green), and local overlap of both (turquoise tones) was visualized in the red fluorescence channel *via* FLIM microscopy after simultaneous excitation at 485 nm and 640 nm.

Paclitaxel assays

Preparation of the nanoparticles

To a solution of P1 or P2, respectively (in acetone, 5 mL, 10 mg·mL⁻¹) containing paclitaxel (250 µg·mL⁻¹), PBS (10.0 mL, containing 0.01 % tween 80) were added as precipitant. The increase in polarity of the solvent led to the aggregation of the polymer chains forming the NPs. The remaining acetone was removed by evaporation and the final volume of the NPs was concentrated to 2.5 mL. Afterwards the NPs solution was washed twice with PBS by using centrifugation/filtration (Amicon 10 kDa – Millipore, Czech Republic). The final PTX concentration was adjusted to 220 µg·mL⁻¹ of PTX (P1) (~ 94 % E.E, HPLC; Fig. S18) and 202 µg·mL⁻¹ of PTX (P2) (~ 92 % E.E, HPLC. Fig. S18). The drug-free NPs were prepared by the same way without adding paclitaxel.

Paclitaxel (PTX) drug loading and loading efficiency

The total amount of the chemotherapeutic PTX loaded into the nanoparticles was measured by high performance liquid chromatography (HPLC, Shimadzu, Japan) using a reverse-phase column Chromolith Performance RP-18e (100 x 4.6 mm), eluent water-acetonitrile with acetonitrile gradient 0-100 vol%, flow rate = 1.0 mL·min⁻¹, as described previously.⁷⁻⁹ The aliquote (100 µL) of drug-loaded NPs was collected from the bulk sample and diluted to 900 µL with acetonitrile. Afterwards, 20 µL of the final sample was injected through a sample loop. PTX was detected at 230 nm using ultraviolet (UV) detection. The retention time of PTX was 12.0 min under such experimental conditions. An analytical curve with linear response in the range 0.5 – 100 µg·mL⁻¹ was obtained and used to determine PTX contents (Fig. S10). The drug-free was separated from the drug-loaded NPs by ultrafiltration-centrifugation (Ultrafree-MC 10,000 MW, Millipore) as detailed elsewhere.¹⁰ The samples were centrifuged at 6000 rpm for 30 min. The free PTX amount was measured in the filtrated after the dissolution of NPs by using acetonitrile as described earlier. The drug-loading content (LC) and the drug-loading efficiency (LE) were calculated by using the following equations:

$$LC(\%) = \frac{\text{drug amount in NPs}}{\text{mass of NPs}} \times 100 \quad (\text{eq. S4})$$

$$LE(\%) = \frac{\text{drug amount in NPs}}{\text{drug feeding}} \times 100 \quad (\text{eq. S5})$$

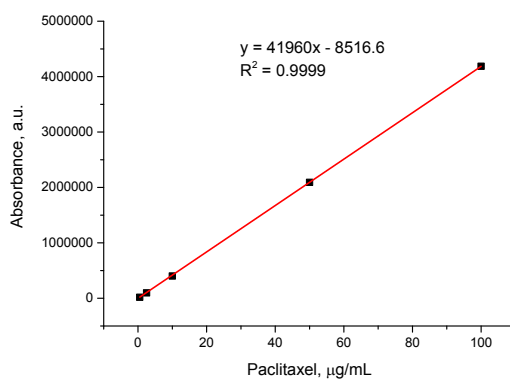


Fig. S18. Calibration curve for paclitaxel.

Paclitaxel release Experiments

The release experiments were carried out at 37 °C in pH-adjusted release media (pH 7.4 and 1 mM of H₂O₂). Aliquots (500 µL) of PTX-NPs were loaded into 36 Slide-A-Lyzer MINI dialysis microtubes with MWCO 10 kDa (Pierce, Rockford, IL). These microtubes were dialyzed against 4 L of PBS (pH 7.4 and 1mM of H₂O₂). The release media was changed periodically to reduce the possibility of drug-diffusion equilibrium (every 12h). The drug release experiments were done in triplicate. At each sampling time, three microtubes were removed from the dialysis system and 0.1 mL from each microtube was diluted to 900 µL with acetonitrile and the sample was ultracentrifuge (18 000 x g, 20 min). Afterwards, 20 µL of the final sample was injected through a sample loop. PTX was detected at 230 nm using ultraviolet (UV) detection using the aforementioned methodologies (Fig. S18). The reported data are expressed as the amount of released PTX relative to the total PTX content in the PTX-NPs.

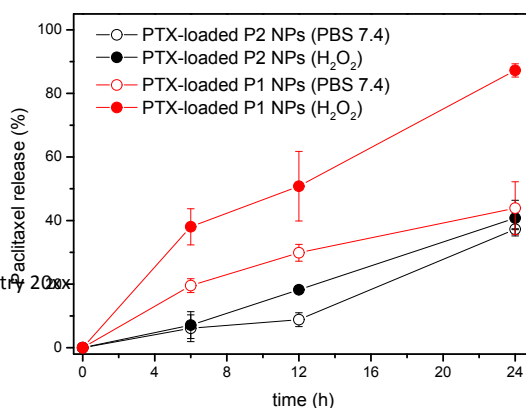


Fig. S19. Paclitaxel (PTX) release from responsive P1 and non-responsive P2 NPs in presence of 1mM of H₂O₂ (filled circles) and in presence of phosphate buffer saline (PBS pH 7.4) (open circles) along 24h incubation at 37 °C.

Cytotoxicity assays

For the cytotoxicity assay, 5000 cells per well (HeLa, DLD1), 7000 (HF) or 10.000 (PC-3), were seeded in duplicates in 96 well plates in 100 μ L of media at least one day (2 days for PC-3) before adding the NPs. For adding of the particles the volume was calibrated to 80 μ L, and 20 μ L of the 5-times concentrated dilution of PTX or particle dispersion were added per well to a final PTX concentration ranging from 10⁻⁵ to 1 μ g·mL⁻¹. All dilutions were made in full incubation medium under thorough mixing of each dilution step. The sample concentrations of the PTX-loaded NPs were adjusted to contain the same total amount of PTX as the samples with free PTX. The cells were incubated with free drug or NPs for 24 h, 48 h (Fig. S20) or 72 h (Fig. 7). In a similar manner, HeLa cells were also incubated for 72 similar to the setup described above, but the cells were incubated medium that contained only 2% serum (Fig. 7). A second control of cells incubated in full medium containing 10% serum proved that the reduced serum content had no toxic side effect on the cells (data not shown). Moreover a test with HeLa cells screening the toxicity after 12h, 24h, 48h, 72h and 96h incubation was done (see Fig. S22). After incubation, in all samples 10 μ L of alamarBlue[®] cell viability reagent (Life Technologies, Czech Republic) were added per well and incubated at least 3 h at 37 °C. The fluorescence of the reduced marker dye was read with a Synergy H1 plate reader (BioTek Instruments, US) at excitation 570 and emission 600 nm. Samples of untreated cell and of cells killed with peroxide were used as samples of 100% and 0% viability, respectively. The shown cell assays data is in average of at least 2 measurements, and was obtained in triplicate well setup. PTX-dilutions in incubation medium were made from a PTX stock solution of 200 μ g·mL⁻¹ in PBS/DMSO (96.5 : 3.5 v/v).¹¹ Precipitation of the hydrophobic PTX out of the cell culture medium can therefore be excluded because the PTX was previously fully dissolved and subsequently diluted in the serum-supplied medium under thorough mixing. The final DMSO concentration in the incubation medium was never above 0.4% and therefore of no consequence.¹²

The non-toxic character of the blank particles without drug was shown by incubation of cells with the blank NPs at the same polymer concentrations as were used for the toxicity tests with PTX-loaded NPs (see Fig. S21, below). This ensured that no toxic effect of the polymer material itself interfered with the viability assay. Non-cancer cells HF as well as one representative cancer cell line, PC-3, were incubated for up to 48h with the applied concentrations of P1 and P2 polymer NPs (drug-free), and with diluted DMSO (without drug).

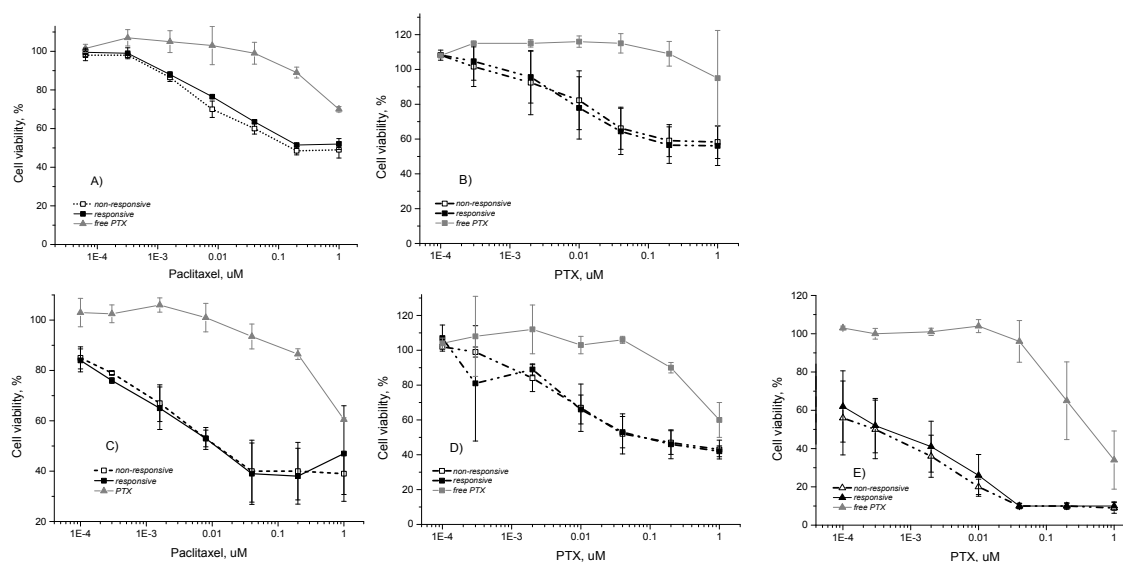


Fig. S20 Incubation of PTX-loaded P1 and P2 NPs with HF (a, c), PC-3 (b, d) and HeLa (e) for 24 h (a, b) and 48 h (c, e). The graphs compare samples with P1 NPs (black, solid symbols), P2 NPs (black, hollow symbols) and free PTX (grey).

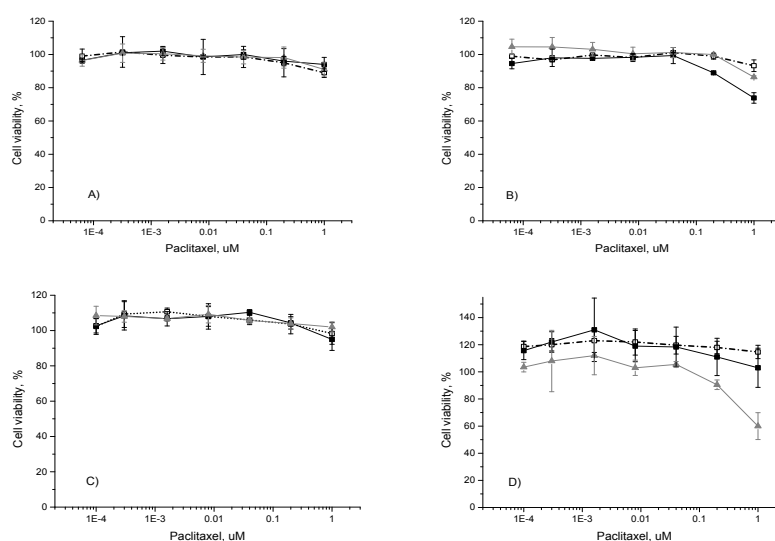


Fig. S21 Control study of the PTX-free NPs in HF (a, b) and PC-3 (c, d) cells. Viability was measured after 24 h (a, c) and 48 h (b, d) of incubation with different concentrations of P2 NPs (open square), ROS-responsive P1 NPs (closed square) and DMSO

(triangle). A maximum concentration of 0.5 (P1 polymer) and 0.6 mg·mL⁻¹ (P2 polymer), and maximal content of 0.4 % DMSO were applied. As these concentrations of DMSO and polymer correspond precisely to those present in the studies with PTX, all graphs are displayed as functions of PTX for convenient comparison.

After 48h incubation at the maximum concentration, minor toxicity of the ROS-responsive polymer NPs (P1) was observed in HF cells, but the effect was also observed in the cancer cells. However, this can be neglected when opposed to the high cell mortality caused by the drug in the respective samples (maximal polymer concentration also corresponds to 1 μM of PTX, which is mortal to both HeLa and HF cells). In another test using HeLa cells, the incubation-dependent toxicity of PTX-loaded NPs was screened and cell viability was measured after 12 h up to 96 h.

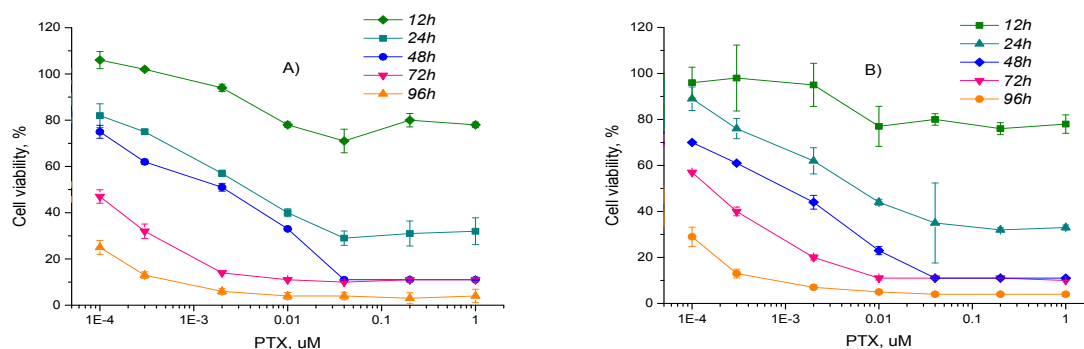


Fig. S22 Incubation of PTX-loaded P1 (a) and P2 (b) NPs with HeLa cells for (from top to bottom) 12h (green), 24h (turquoise), 48h (blue), 72h (pink) and 96h (orange).

The test showed that the PTX-loaded NPs reduced cell viability beneath 50% after 24h incubation time; first toxic effects were even visible after 12 h. The toxicity of the drug-loaded ROS-sensitive NPs (P1) increased steeply when incubation time was raised up to 96 h. At all times the particle toxicity was significantly above that of the free drug (data not shown). The non-responsive NPs (P2) showed similar efficient killing of the cells as the P1 NPs responsive NPs. However, especially at longer incubation > 48 h, the test indicated a higher efficiency of the ROS-responsive system (P1 NPs). With HeLa cells as an aggressive cancer cell line comparable to PC-3 this test indicated a selective, ROS-induced cargo release from P1 NPs in the cells.

References

- [1] C. de G. Lux, S. Joshi-Barr, T. Nguyen, E. Mahmoud, E. Schopf, N. Fomina and A. Almutairi, *J. Am. Chem. Soc.*, 2012, **134**, 15758.
- [2] P. Štěpánek, In *Dynamic light scattering: The Method and Some Applications*; Brown, W., Ed.; Oxford Science Publications: Oxford, 1993.
- [3] J. Panyam and V. Labhasetwar, *Pharm. Res.*, 2003, **2**, 20.
- [4] A. Cser, K. Nagy and L. Biczók, *Chem. Phys. Lett.*, 2002, **360**, 473.
- [5] A.-Y. Jee, S. Park, H. Kwon and M. Lee, *Chem. Phys. Lett.*, 2009, **477**, 112.
- [6] A.K. Dutta, K. Kamada and K. Ohta, *J. Photochem. Photobiol. A Chem.*, 1996, **93**, 57.
- [7] F.C. Giacomelli, P. Štěpánek, C. Giacomelli, V. Schmidt, E. Jäger, A. Jäger and K. Ulbrich, *Soft Matter* 2011, **7**, 9316.
- [8] A. Jäger., D. Gromadzki, E. Jäger, F.C. Giacomelli, A. Kozłowska, L. Kobera, J. Brus, B. Říhová, M. El Fray, K. Ulbrich, P. Štěpánek, *Soft Matter* 2012, **8**, 4343.
- [9] A. Jäger., E. Jäger, F. Surman, A. Höcherl, A. Angelov, K Ulbrich, M. Dreschler, V.M. Garamus, C. Rodriguez-Emmenegger, F. Nallet, P. Štěpánek, *Polym. Chem.*, 2015, **8**, 4343.
- [10] E. Penott-Chang, A. Walther, P. Millard, A. Jäger, E. Jäger, A.H.E. Müller, S.S. Guterres, A.R. Pohlmann, *J. Biomed. Nanotechnol.*, 2012, **8**, 272.
- [11] E.A. Dubikovskaya, S.H. Thorne, T.H. Pillow, C.H. Contag and P.A. Wender. *Proc. Natl. Acad. Sci. U.S.A* 2008, **105**, 12128.
- [12] A. B. Trivedi, N. Kitabatake, E. Do. *Agr. Biol. Chem.*, 1990, **54**, 2961.
-